New iodine-rich Group 15 iodometalates(III): self-assembly of metal halide anions and polyiodides into supramolecular architectures via I···I Contacts

Irina A. Shentseva, Nikita A. Korobeynikov, Andrey N. Usoltsev, Maxim N. Sokolov and Sergey Adonin*

Powder X-ray diffractometry (PXRD)

Analysis of polycrystals was performed on Bruker D8 Advance (CuK_α radiation, LYNXEYE XE-T linear detector, 4 – 50° 2θ range, 0.03° 2θ step, 0.5s per step) and Shimadzu XRD-7000 diffractometer (CuKα radiation, Ni – filter, linear One Sight detector, 5 – 50° 2θ range, 0.0143° 2θ step, 2s per step). A polycrystalline sample was slightly ground with hexane in an agate mortar, and the resulting suspensions were deposited on the polished side of a standard quartz sample holder, and a smooth thin layer being formed after drying. The diffraction patterns of **1-2** were completely indexed by the results of the corresponding single crystal studies, and no extra lines were found, which indicated that the products were a single phase.

Raman spectra were collected using a LabRAM HR Evolution (Horiba) spectrometer with the excitation by the 633 nm line of the He-Ne laser. The spectra at room temperatures were obtained in the backscattering geometry with a Raman microscope. The laser beam was focused to a diameter of 2 μm using a LMPlan FL 50x/0.50 Olympus objective. The spectral resolution was 0.7 cm^{-1}. The laser power on the sample surface was about 0.03 mW.

Thermogravimetric analysis (TGA) of **1-2** were carried out on a TG 209 F1 Iris thermobalance (NETZSCH, Germany). The measurements were made in a helium flow in the temperature range of 30–450°C using the heating rate of 10°C/min the gas flow rate of 60 mL/min and open Al crucibles.

Diffuse reflectance spectra of **1-2** were measured on a setup which consists of a Kolibri-2 spectrometer (VMK Optoelektronica, Russia), fiber optic cable QR-400-7 (Ocean Optics, USA), and deuterium–tungsten lamp AvaLight-DHS (Avantes, Netherlands). The reference of 100% reflectance was $BaSO_4$ powder. The spectra were recorded five times in the wavelength interval of 300-1000 nm and then averaged to reduce the random error.

Table S1. Crystal data and structure refinement for **1**–**2**.

Identification code	**1**	**2**
Empirical formula	$C_{78}H_{105}I_{33}N_{12}O_4Sb_4$	$C_{78}H_{105}I_{33}N_{12}O_4Bi_4$
M, g/mol	5949.43	6298.35
Temperature/K	150	150
Crystal system	Monoclinic	Monoclinic
Space group	*C2*	*C2/c*
a, Å	16.9204 (3)	16.913 (2)
b, Å	14.3689 (3)	14.4492 (17)
c, Å	29.1546 (7)	56.667 (7)
α, deg.	90	90
β, deg.	105.236 (1)	91.534 (4)
γ, deg.	90	90
Volume, Å^3	6839.1 (3)	13843 (3)
Z	2	4
ρ_{calc}, g/cm^3	2.889	3.022
μ, mm^{-1}	8.27	12.47
F(000)	5284	11080
Crystal size, mm	0.07 × 0.05 × 0.02	0.08 × 0.06 × 0.02
Θ range for data collection, deg.	1.888 to 33.154	1.854 to 31.524
Tmin, Tmax	0.609, 0.747	0.526, 0.746
Range of h, k, l	-24 ≤ h ≤ 26, -22 ≤ k ≤ 22, -44 ≤ l ≤ 44	-14 ≤ h ≤ 24, -21 ≤ k ≤ 20, -82 ≤ l ≤ 82
$(\sin\theta/\lambda)_{max}$ (Å^{-1})	0.769	0.736
R_{int}	0.068	0.053
Reflections collected/independent	74686, 25992	76995, 22931
Reflections with I > 2σ(I)	18188	16449
Data/restraints/parameters	25992/1/633	22931/7/613
Goodness-of-fit on F^2	1.019	1.051
Final R indexes [I>=2σ (I)]	R_1 = 0.0505, wR_2 = 0.0719	R_1 = 0.0437, wR_2 = 0.0794
Final R indexes [all data]	R_1 = 0.0842, wR_2 = 0.0856	R_1 = 0.0682, wR_2 = 0.0874
Weighting scheme	w =1/[σ^2(F$_o^2$)+(0.0167P)^2] where P = (F$_o^2$ + 2F$_c^2$)/3	w =1/[σ^2(F$_o^2$)+ 172.5404P] where P = (F$_o^2$ + 2F$_c^2$)/3
$(\Delta/\sigma)_{max}$	0.001	0.004
Largest diff. peak/hole, e/Å^3	1.69, −1.37	1.83, −1.84

Computer programs: SHELXT 2014/5 (Sheldrick, 2014), SHELXL 2017/1 (Sheldrick, 2015), Olex2 1.5 (Dolomanov et al., 2009).

Table S2. Selected bond lengths and angles for **1**.

Bond length, Å			
I5—Sb1	3.0499 (8)	I16—I17	2.9303 (9)
Sb2—I12	2.8280 (9)	I16—I15	2.9322 (9)
Sb2—I10	2.9035 (8)	I2—Sb1	2.8532 (8)
Sb2—I14A	3.1789 (6)	I4—Sb1	3.0195 (15)
Sb2—I13A	2.9871 (16)	Sb1—I3	2.9729 (9)
Sb2—I11A	3.099 (5)	Sb1—I1	3.0111 (15)
Sb2—I14B	3.222 (4)	I6—I7	3.0605 (9)
Sb2—I13B	2.797 (17)	I7—I8	2.8201 (10)
Sb2—I11B	3.18 (3)		
Bond angle, (°)			
I12—Sb2—I10	89.94 (3)	I13B—Sb2—I14B	96.7 (5)
I12—Sb2—I14A	92.53 (2)	I13B—Sb2—I11B	175.8 (10)
I12—Sb2—I13A	87.54 (5)	I11B—Sb2—I14B	79.4 (7)
I12—Sb2—I11A	87.78 (8)	I17—I16—I15	178.52 (3)
I12—Sb2—I14B	91.24 (5)	I2—Sb1—I5	91.23 (2)
I12—Sb2—I11B	82.1 (13)	I2—Sb1—I4	90.78 (4)
I10—Sb2—I14A	177.47 (3)	I2—Sb1—I3	91.94 (2)
I10—Sb2—I13A	92.06 (4)	I2—Sb1—I1	91.01 (4)
I10—Sb2—I11A	90.13 (10)	I4—Sb1—I5	90.29 (4)
I10—Sb2—I14B	167.3 (4)	I3—Sb1—I5	176.84 (3)
I10—Sb2—I11B	88.2 (5)	I3—Sb1—I4	89.72 (4)
I13A—Sb2—I14A	87.48 (5)	I3—Sb1—I1	89.67 (4)
I13A—Sb2—I11A	174.83 (9)	I1—Sb1—I5	90.23 (4)
I11A—Sb2—I14A	90.53 (11)	I1—Sb1—I4	178.12 (3)
I13B—Sb2—I12	99.5 (5)	Sb2—I14A—Sb2^{i}	173.34 (9)
I13B—Sb2—I10	95.6 (3)	I8—I7—I6	177.46 (4)

Symmetry code(s): (i) $-x+2, y, -z+1$.

Table S3. Selected bond lengths and angles for **2**.

Bond lengths, Å			
Bi2—I12	2.9106 (6)	Bi1—I2	2.9365 (6)
Bi2—I10	2.9690 (5)	Bi1—I5	3.0902 (6)
Bi2—I9A	3.2417 (7)	Bi1—I4	3.0702 (6)
Bi2—I14A	3.2113 (4)	Bi1—I1	3.0818 (6)
Bi2—I13A	3.1403 (7)	Bi1—I3	3.0333 (6)
Bi2—I11A	3.0722 (7)	Bi1—I6	3.3434 (5)
Bi2—I9B	3.306 (9)	I6—I7	3.0734 (8)
Bi2—I14B	3.243 (4)	I7—I8	2.8163 (8)
Bi2—I11B	2.899 (9)	I15—I16	2.9318 (7)
Bi2—I13B	3.366 (12)	I16—I17	2.9306 (7)
Bond angles, (°)			
I12—Bi2—I10	89.981 (16)	I11B—Bi2—I10	96.0 (2)
I12—Bi2—I9A	172.869 (15)	I11B—Bi2—I9B	103.6 (4)
I12—Bi2—I14A	92.939 (14)	I11B—Bi2—I14B	95.4 (5)
I12—Bi2—I13A	87.671 (19)	I11B—Bi2—I13B	174.3 (4)
I12—Bi2—I11A	87.413 (19)	Bi2^{ii}—I14A—Bi2	172.50 (5)
I12—Bi2—I9B	157.30 (16)	Bi2^{ii}—I14B—Bi2	162.4 (8)
I12—Bi2—I14B	91.61 (5)	I2—Bi1—I5	91.824 (16)
I12—Bi2—I13B	76.1 (3)	I2—Bi1—I4	91.363 (14)
I10—Bi2—I9A	85.374 (16)	I2—Bi1—I1	91.370 (14)
I10—Bi2—I14A	176.993 (15)	I2—Bi1—I3	92.083 (16)
I10—Bi2—I13A	90.891 (15)	I2—Bi1—I6	176.119 (15)
I10—Bi2—I11A	92.687 (14)	I5—Bi1—I6	92.050 (15)
I10—Bi2—I9B	84.21 (16)	I4—Bi1—I5	90.342 (14)
I10—Bi2—I14B	168.1 (4)	I4—Bi1—I1	177.148 (15)
I10—Bi2—I13B	86.8 (2)	I4—Bi1—I6	88.378 (14)
I14A—Bi2—I9A	91.651 (14)	I1—Bi1—I5	90.384 (13)
I13A—Bi2—I9A	97.793 (18)	I1—Bi1—I6	88.840 (13)
I13A—Bi2—I14A	89.94 (3)	I3—Bi1—I5	176.092 (14)
I11A—Bi2—I9A	87.403 (19)	I3—Bi1—I4	89.515 (14)
I11A—Bi2—I14A	86.73 (3)	I3—Bi1—I1	89.573 (14)
I11A—Bi2—I13A	173.92 (2)	I3—Bi1—I6	84.043 (15)
I9B—Bi2—I13B	81.6 (3)	I7—I6—Bi1	144.03 (2)
I14B—Bi2—I9B	89.8 (2)	I8—I7—I6	176.94 (2)
I14B—Bi2—I13B	82.1 (5)	I17—I16—I15	178.70 (2)
I11B—Bi2—I12	98.9 (3)		

Symmetry code(s): (i) $x+1/2, y-1/2, z$; (ii) $-x+1, y, -z+3/2$.

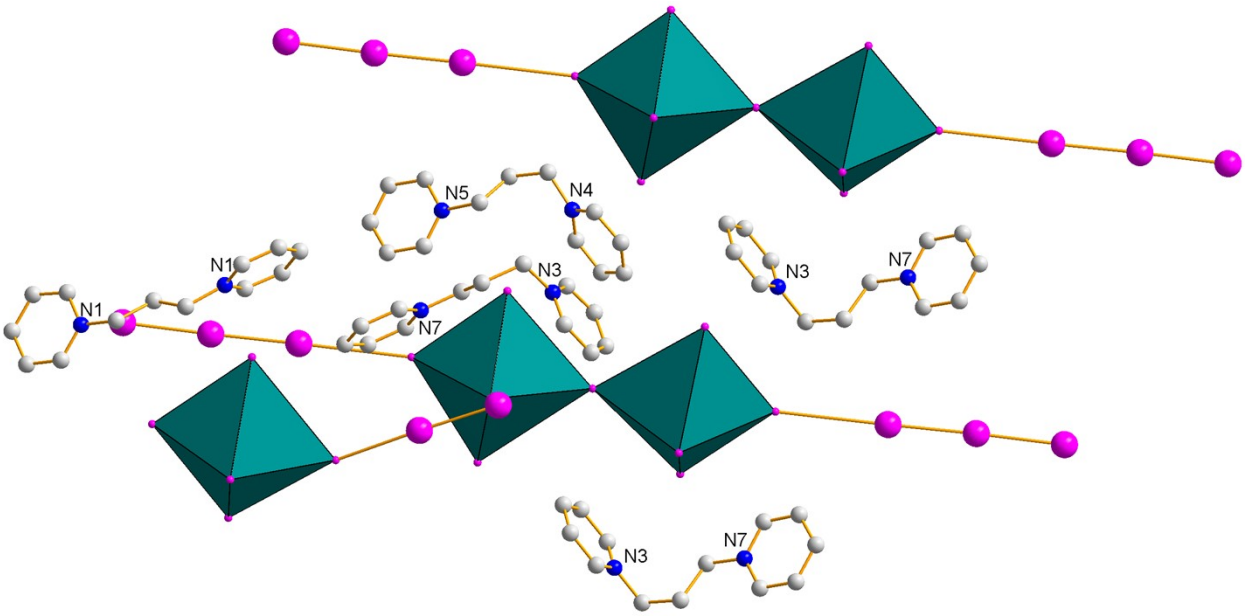

Figure S1. Fragment of crystal structure of **1** with two different types of anions (conformation with nitrogen atoms denoted N1 and *tg* with N3, N4, N5 and N7.

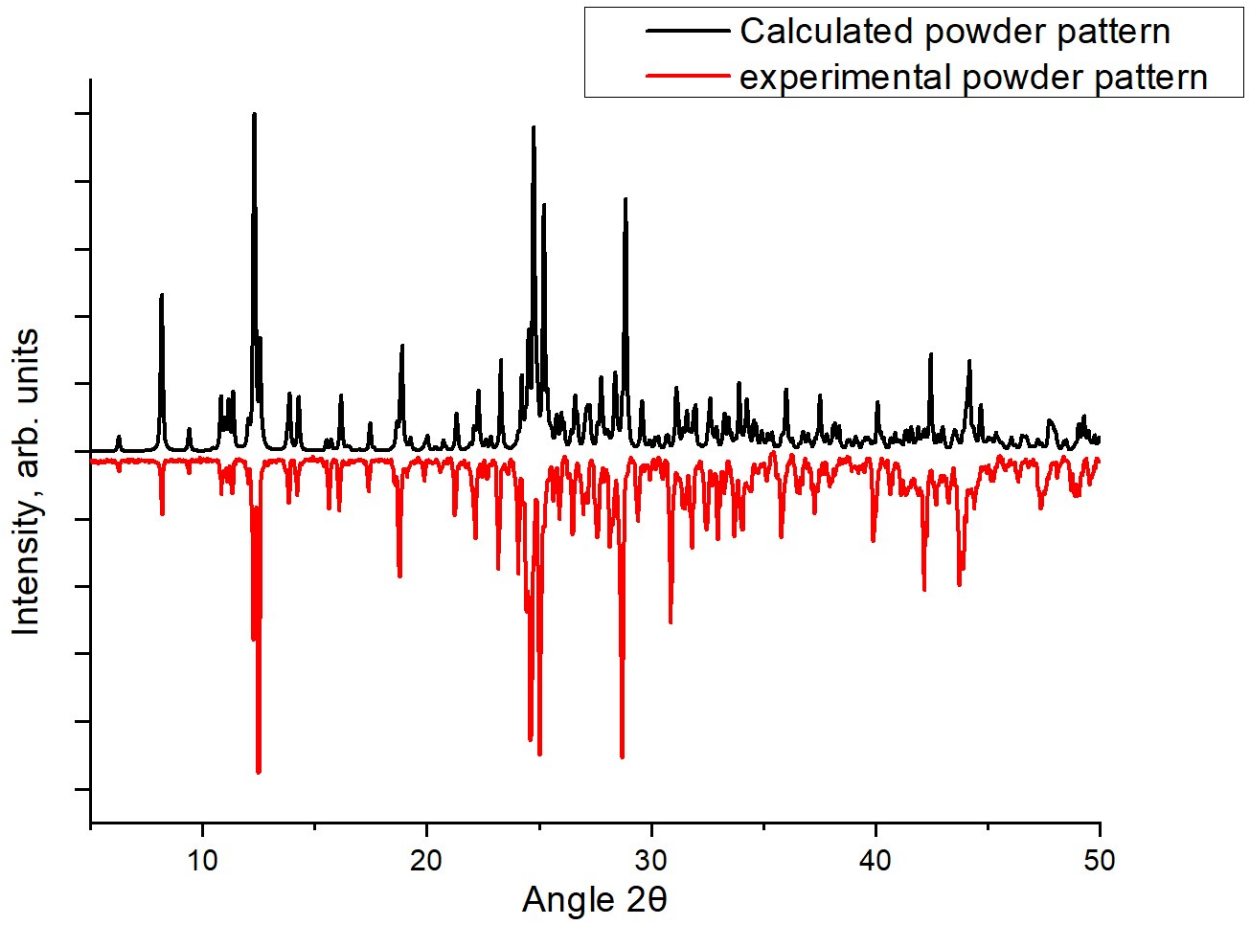

Figure S2. Theoretical and experimental PXRD patterns for **1**.

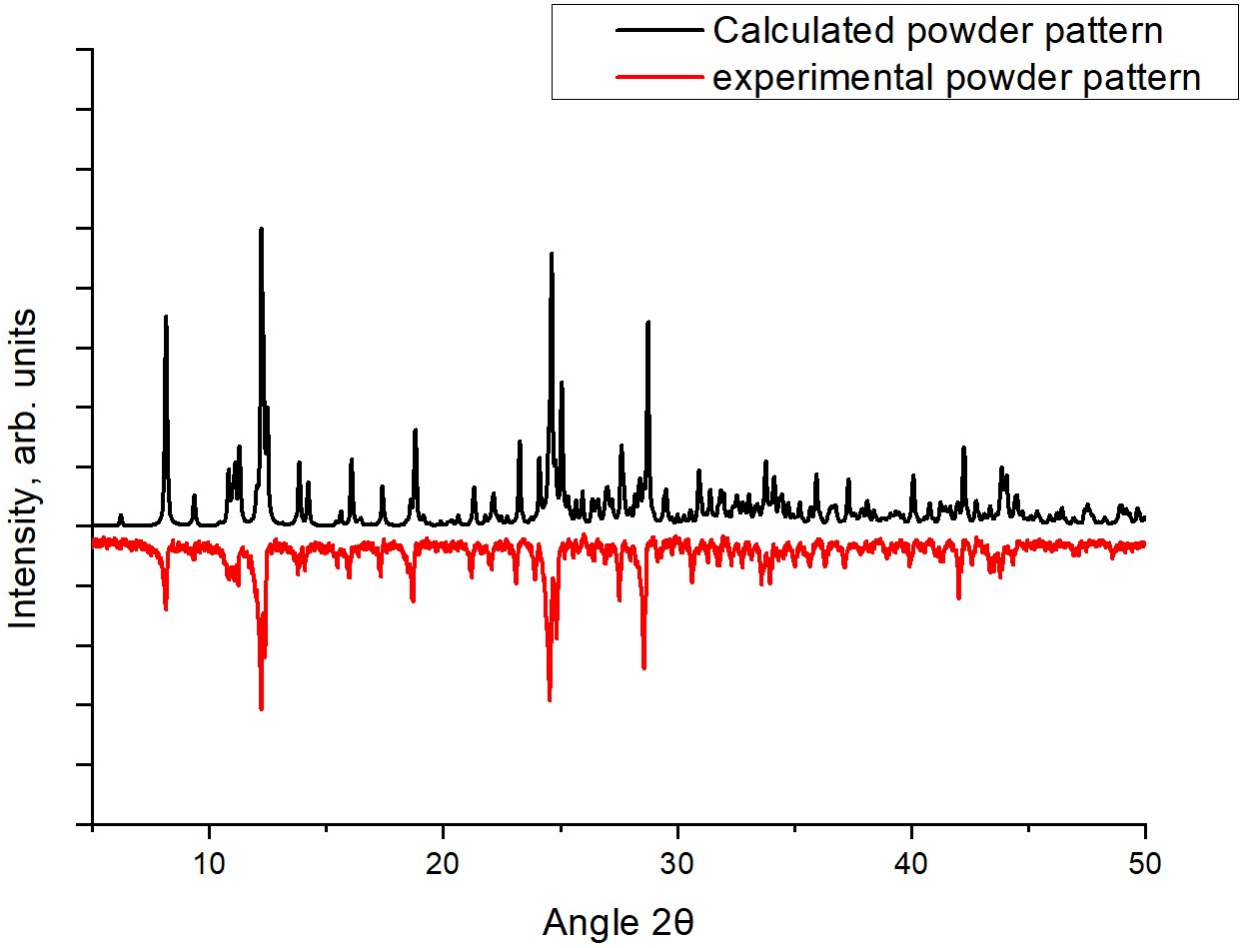

Figure S3. Theoretical and experimental PXRD patterns for **2**.

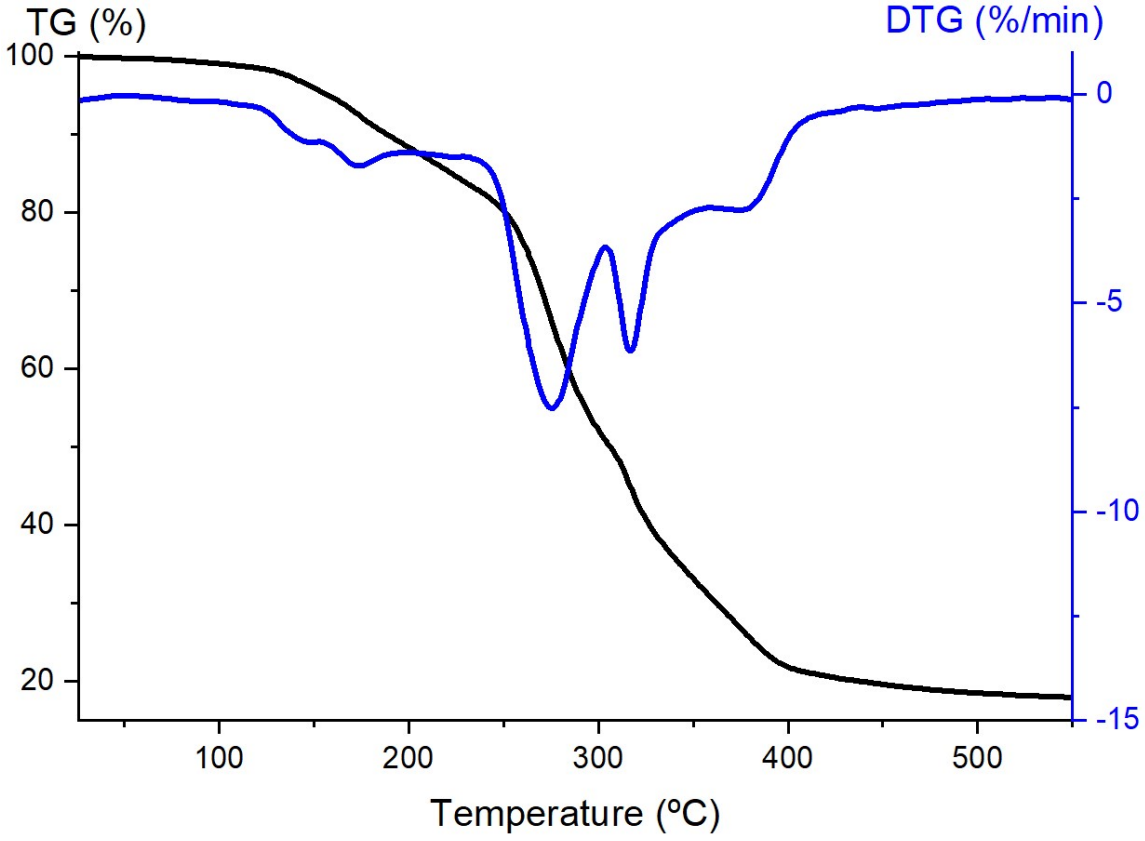

Figure S4. TG, DTG and DTA curves for **2**.

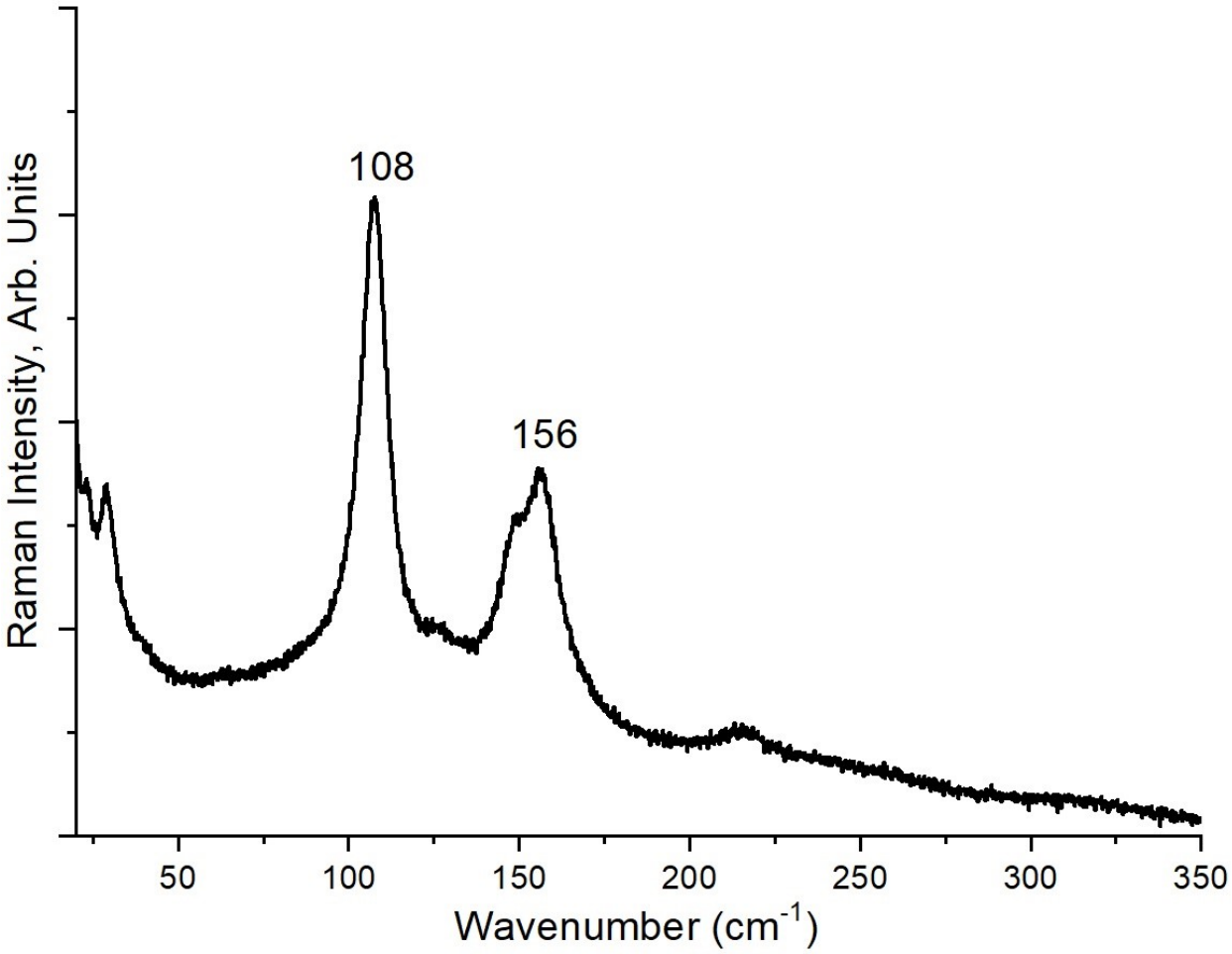

Figure S5. Raman spectrum of **1**.

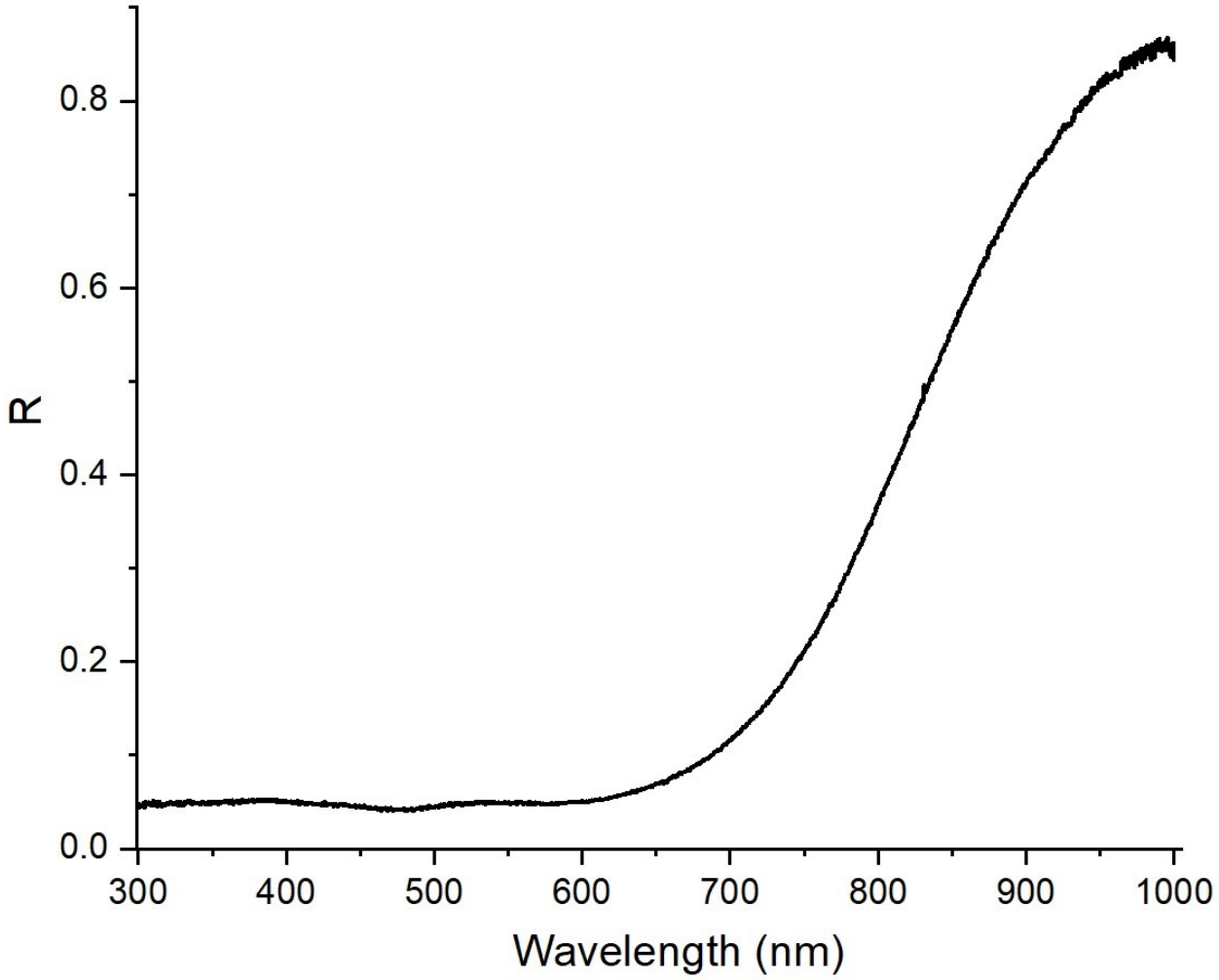

Figure S6. Diffuse reflectance spectrum of **1**.

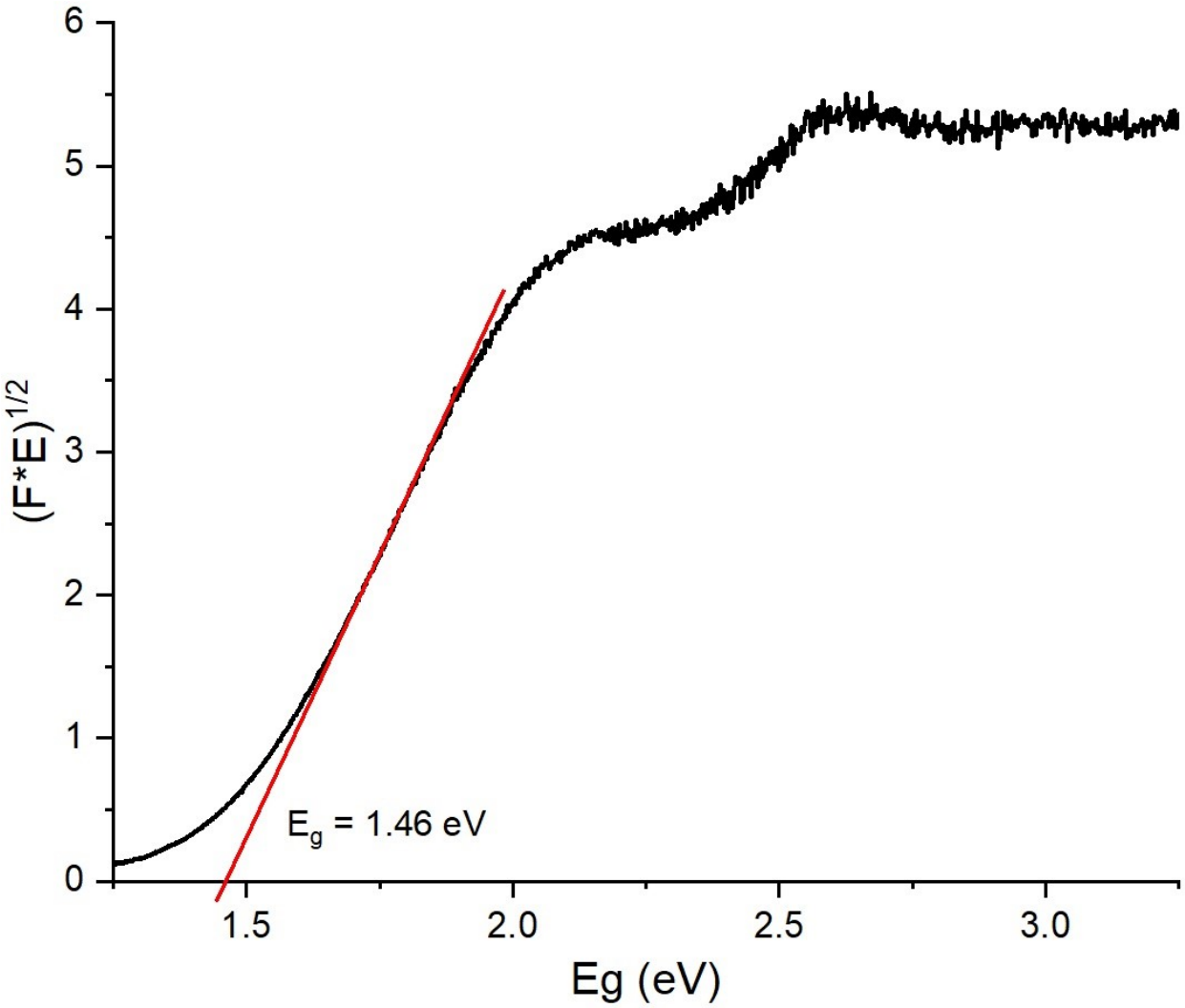

Figure S7. Optical bandgap determination via Tauc coordinates for **1**.